

# Robust retrofitting design for rehabilitation of segmental tunnel linings

Zhang, Dong-ming; Zhai, Wu-zhou; Huang, Hong-wei; Chapman, David

DOI:

[10.1016/j.tust.2018.09.016](https://doi.org/10.1016/j.tust.2018.09.016)

License:

Creative Commons: Attribution-NonCommercial-NoDerivs (CC BY-NC-ND)

*Document Version*

Peer reviewed version

*Citation for published version (Harvard):*

Zhang, D, Zhai, W, Huang, H & Chapman, D 2019, 'Robust retrofitting design for rehabilitation of segmental tunnel linings: using the example of steel plates', *Tunnelling and Underground Space Technology*, vol. 83, pp. 231-242. <https://doi.org/10.1016/j.tust.2018.09.016>

[Link to publication on Research at Birmingham portal](#)

**Publisher Rights Statement:**

Checked for eligibility: 23/10/2018

**General rights**

Unless a licence is specified above, all rights (including copyright and moral rights) in this document are retained by the authors and/or the copyright holders. The express permission of the copyright holder must be obtained for any use of this material other than for purposes permitted by law.

- Users may freely distribute the URL that is used to identify this publication.
- Users may download and/or print one copy of the publication from the University of Birmingham research portal for the purpose of private study or non-commercial research.
- User may use extracts from the document in line with the concept of 'fair dealing' under the Copyright, Designs and Patents Act 1988 (?)
- Users may not further distribute the material nor use it for the purposes of commercial gain.

Where a licence is displayed above, please note the terms and conditions of the licence govern your use of this document.

When citing, please reference the published version.

**Take down policy**

While the University of Birmingham exercises care and attention in making items available there are rare occasions when an item has been uploaded in error or has been deemed to be commercially or otherwise sensitive.

If you believe that this is the case for this document, please contact [UBIRA@lists.bham.ac.uk](mailto:UBIRA@lists.bham.ac.uk) providing details and we will remove access to the work immediately and investigate.

1       **Robust Retrofitting Design for Rehabilitation of Segmental Tunnel Linings:**

2                               **Using the Example of Steel Plates**

3               Dong-ming Zhang<sup>a</sup>, Wu-zhou Zhai<sup>b</sup>, Hong-wei Huang<sup>c,\*</sup>, David Chapman<sup>d</sup>

4       <sup>a</sup> Assistant Professor, Key Laboratory of Geotechnical and Underground Engineering  
5       of Minister of Education and Department of Geotechnical Engineering, Tongji  
6       University, Shanghai, China. [09zhang@tongji.edu.cn](mailto:09zhang@tongji.edu.cn)

7       <sup>b</sup> Ph.D candidate, Key Laboratory of Geotechnical and Underground Engineering of  
8       Minister of Education and Department of Geotechnical Engineering, Tongji  
9       University, Shanghai, China. [zhaiwuzhou@tongji.edu.cn](mailto:zhaiwuzhou@tongji.edu.cn)

10       <sup>c</sup> Professor, Key Laboratory of Geotechnical and Underground Engineering of  
11       Minister of Education and Department of Geotechnical Engineering, Tongji  
12       University, Shanghai, China. [huanghw@tongji.edu.cn](mailto:huanghw@tongji.edu.cn)

13       <sup>b</sup> Professor, School of Civil Engineering, College of Engineering and Physical  
14       Sciences, University of Birmingham, Edgbaston, Birmingham, UK.  
15       [d.n.chapman@bham.ac.uk](mailto:d.n.chapman@bham.ac.uk)

16

17

18 **Robust Retrofitting Design for Rehabilitation of Segmental Tunnel Linings:**

19 **Using the Example of Steel Plates**

20

21 **Abstract:** This paper presents a general framework for the robust retrofitting design  
22 for rehabilitation of segmental tunnel linings installed using shield tunnelling, and  
23 specifically using steel plates bonded to the lining as a typical example of such a  
24 rehabilitation design. A two-dimensional finite element model is established as part of  
25 the robust design which can simulate the deformational response of the steel plates  
26 reinforced segmental tunnel lining. The surrounding soil, the tunnel lining, the steel  
27 plates and the interactions between each of these are all properly simulated in this  
28 model and verified by full-scale test results. The change in horizontal convergence  
29 ( $\Delta D_{hs}$ ) subjected to environmental impact, such as unexpected placement of ground  
30 surface surcharge is measured to reflect the performance of segmental tunnel linings  
31 reinforced by steel plates. The standard deviation of the reinforced tunnel  
32 performance due to uncertainties in the soil conditions and the ground surface  
33 surcharge is derived to measure the design robustness. A robust rehabilitation design  
34 is then accomplished by varying the steel plates sizes (i.e. width and thickness) to  
35 maximize the design robustness and minimize the cost using a multi-objective  
36 algorithm, also considering the safety requirement constraints. The optimal designs  
37 are determined as a set of design points, namely a Pareto Front, which presents a  
38 trade-off relationship between the design objectives and is demonstrated as being

39 useful for decision making. Finally, the robust rehabilitation design method is applied  
40 to the retrofitting design of tunnel lining using steel plates in a real case study, and a  
41 comparison between the actual design and the design derived by the proposed method  
42 has been made to show its applicability and potentially significant advantages for  
43 designers, as the method allows consideration of both the highest robustness and the  
44 lowest cost simultaneously.

45 **Key words:** Robust design, segmental tunnel lining, steel plates, uncertainties,  
46 decision making

## 47 **1. Introduction**

48 The worldwide long-term development of urban metro system has driven the wide  
49 use of shield tunneling in construction especially in soft ground. Hence, segmentally  
50 lined tunnels installed by shield tunnelling have been utilized for decades, for example  
51 London, Tokyo and Shanghai. However, as a typically prefabricated assembled  
52 concrete structure, a segmental tunnel lining is vulnerable to nearby disturbance  
53 especially in soft ground conditions such as those experienced in Shanghai. Large  
54 deformation in terms of transverse convergence and longitudinal settlement, and the  
55 associated severe structural defects such as leakage, concrete cracking and spalling  
56 have been detected in segmentally lined tunnels from on-site inspection and  
57 monitoring data (Shi and Li, 2015; Yuan et al., 2013). The structural health of  
58 segmental linings are likely to be adversely affected by nearby engineering activities  
59 and human-error related hazards. A typical example was reported by Huang et al.  
60 (2017) for a field case study involving an extreme surcharge being applied to a

61 running metro tunnel in Shanghai. Therefore effective rehabilitation treatments for  
62 distressed concrete segmental linings are of great importance, especially at this time  
63 of rapid development of shield tunnel construction.

64 There are several methods suitable for repairing and strengthening segmental tunnel  
65 linings, for example bonding fiber reinforced polymer (FRP) or steel plates to the  
66 inner surface of segmental concrete linings (Liu and Zhang, 2014; Kiriyaama et al.,  
67 2005), and grouting on either side of the tunnel at its spring line (Zhang et al., 2014).  
68 From these repair measures, bonding steel plates to an existing lining is often chosen  
69 as a permanent strengthening method. This rehabilitation approach using bonded steel  
70 plates can potentially enhance both the structural stiffness and the ultimate capacity  
71 (Kiriyaama et al., 2005). Furthermore, the construction operations associated with  
72 bonding steel plates can rely on standard machinery resulting in a fast and effective  
73 repair procedure. Hence, bonding the steel plates has been successfully adopted as a  
74 permanent rehabilitation method in many projects involving damaged segmental  
75 tunnel linings worldwide (Chang et al., 2001; Huang and Zhang, 2016).

76 Kiriyaama et al. (2005) presented an analytical analysis for the design of steel plate  
77 reinforcement for existing deformed tunnels utilizing a beam spring model. In the  
78 model, the steel plates are modelled as a circumferential beam, and a series of  
79 nonlinear springs with no tensile resistance are applied in the radial direction to  
80 simulate the interaction. Based on the practice of steel plate reinforcement frequently  
81 used in Shanghai, Zhao et al. (2015) conducted a full scale load test on a steel plate  
82 reinforced segmental lining ring. In their study, a simplified numerical model was

83 established to further investigate the mechanical and deformational behaviour of  
84 reinforced tunnel linings. Apart from these researchers providing insight into the  
85 structural response of the lining, other research has focused on the bonding behaviour  
86 and failure mode of epoxy bonded steel plate reinforcing concrete structures ([Ziraba](#)  
87 [et al., 1995](#); [Adhikary et al., 2002](#)). Previous literature on numerical simulations  
88 provide a basic understanding of the effectiveness of bonding steel plates on the  
89 disrupted tunnel structures. However, the model used previously simplified the  
90 behaviour of the surrounding soils by using soil springs based on Winkler's model  
91 ([Do, et al., 2015](#); [Zhang et al., 2017](#)). This simplification will further contribute to any  
92 discrepancy between the prediction and the field measurements, especially when the  
93 ground conditions are very uncertain in the context of soil properties. Furthermore,  
94 the design of steel plate rehabilitation mainly depends on the engineering experience.  
95 Hence, an appropriate design model for the rehabilitation of segmental tunnel linings  
96 that can be robust appropriate for the environmental uncertainty would be extremely  
97 welcome.

98 A robust design methodology was originally developed by [Taguchi & Wu \(1979\)](#)  
99 for improving the industrial product quality and manufacturability. Since then a great  
100 many studies have been conducted to understand this idea and make it applicable to  
101 other areas. The main idea behind a robust design is to make the system response  
102 insensitive to (robust against) hard-to-control disturbances (called noise factors) at a  
103 low cost ([Kwokleung, 2007](#)). Based on this concept, some researchers have put effort  
104 into robust designs of various kinds of structural systems under different uncertainties

105 (Doltsinis and Zhan, 2004; Beer and Liebscher, 2008). In contrast to the design of  
106 structures, the geotechnical uncertainty may significantly influence the design  
107 associated with geotechnical problems (Phoon and Kulhawy, 1999). Recently, Juang  
108 and Wang (2013) proposed a robust geotechnical design (RGD) methodology and  
109 applied it to different forms of geotechnical problems such as spread foundations,  
110 drilled shafts (Juang et al., 2013) and braced excavations (Juang, et al., 2014). Gong et  
111 al. (2014) have applied the robustness design concept for the design of segmental  
112 tunnel linings, the idea of this robust design model is to reduce the variation of tunnel  
113 lining performance under normal conditions caused by the uncertainty of the input  
114 design parameters.

115 The aim of this paper is to present a general framework for the rehabilitation design  
116 for segmental linings from shield tunnelling under the conceptual umbrella of  
117 robustness. The goal of robust retrofitting design is to enhance the robustness of the  
118 reinforced segmental linings against the design uncertainties with consideration given  
119 to minimizing cost, which can be accomplished by varying the design parameters to  
120 minimize the variation of the reinforced segmental tunnel lining performance given  
121 some uncertainty level of the surrounding environments. The general framework for a  
122 robust design model is presented first. Secondly a two-dimensional finite element  
123 model is established to simulate the steel-plate-reinforced segmental tunnel lining for  
124 the design. The interactions between the steel plates and the lining and also between  
125 the lining and the surrounding ground are carefully modelled and verified by  
126 full-scale load test results. Finally, a detailed design example is carried out

127 demonstrating the applicability of proposed robust design methodology for the  
128 rehabilitation of segmental tunnel linings using steel plates.

## 129 **2. Framework of robust retrofitting design for segmental tunnel linings**

### 130 **2.1 Practical design method of steel plate strengthening**

131 Figure 1 presents a photograph showing segmental tunnel linings strengthened  
132 by steel plates in the Shanghai metro. The steel plates were installed separately and  
133 welded together to form an integral ring. Epoxy was injected into the gap and to  
134 provide a bond between the lining and the steel plates. Due to the complexity and  
135 potentially large differences between the damaged tunnel conditions from case to case,  
136 there isn't a common design method for the steel plate rehabilitation method. In fact,  
137 the steel plates are usually only applied to damaged tunnel linings with a horizontal  
138 convergence of over 10cm. The size of the steel plates used is nearly the same in each  
139 case based on past engineering experience, having a width of 850mm and a thickness  
140 of 20~30mm. Although this may be convenient in practice, there is certainly room for  
141 improvement and optimization in the design of steel plate reinforcement for particular  
142 cases.

### 143 **2.2 Robust retrofitting design methodology**

144 In the robust rehabilitation design procedure, it is aimed to find an appropriate  
145 set of design parameters, which makes the performance of reinforced tunnel lining  
146 robust enough with the lowest possible total cost. The horizontal convergence is  
147 widely adopted as an indicator of tunnel lining performance both in the research field  
148 and in engineering practice (Huang and Zhang, 2016). In this study, the change in



149 horizontal convergence ( $\Delta D_{hs}$ ) as a result of an environmental impact such as an  
150 unexpected ground surface surcharge, compared to the horizontal convergence  $\Delta D_{h0}$   
151 just after the steel plate installation has finished is measured to reflect the performance  
152 of segmental tunnel lining reinforced by steel plates. However, the change in the  
153 convergence  $\Delta D_{hs}$  as a result of a changed environment will be dependent on multiple  
154 sources of uncertainties, for examples the ground properties and the surcharge levels,  
155 while the degree of variation in  $\Delta D_{hs}$  can be quantified by its standard deviation to  
156 show how sensitive the reinforced segmental tunnel lining is to the noise factors  
157 (Juang et al., 2014).

158 Therefore, the goal of proposed robust retrofitting design is to enhance the  
159 robustness of the reinforced segmental tunnel lining against the design uncertainties at  
160 low cost, which can be accomplished by varying the design parameters to minimize  
161 the standard deviation of the reinforced tunnel performance,  $\Delta D_{hs}$ , given some  
162 uncertainty levels of the surrounding environments. As shown in the flowchart in Fig.  
163 3, the robust rehabilitation design procedure is summarized as follows:

164 Step 1: The problem should initially be defined, with the input parameters being  
165 divided into two categories, namely the design parameters (*easy to control* factors)  
166 and the *noise* factors (*hard to control* factors) (Kwokleung, 2007). The sizes of the  
167 steel plates, such as width ( $w_s$ ) and thickness ( $t_s$ ) are adopted as the design parameters,  
168 as these can be specified by the designers. The *noise* factors are the properties of  
169 ground such as soil Young's modulus ( $E$ ) and environmental impacts, such as the  
170 ground surface surcharge ( $P$ ) in relation to the long-term service life after

171 rehabilitation.

172 Step 2: The uncertainty of the *noise* factors is characterized and the domain of  
173 the design parameters is defined. In this study, the uncertainty of these noise factors  
174 (i.e.  $E$  &  $P$ ) can be characterized using the data from site investigation information  
175 and engineering experience. The domain of the design parameters (i.e.  $w_s$  &  $t_s$ ) is  
176 specified by the lower and upper bounds of each design parameters, which can be  
177 assigned according to the lining segment dimensions, the limitations of tunnel gauge  
178 and engineering experience.

179 Step 3: However, calculating the deformation of the steel-plate-reinforced  
180 segmental tunnel lining cannot be solved analytically given the complex interaction  
181 problems, and requires numerical simulations. A particular numerical model is  
182 established which can simulate the accurate structural response of segmental tunnel  
183 linings reinforced by steel plates given certain values of input parameters. The  
184 proposed numerical model will be introduced in detail later.

185 In reality, the steel plates are often applied to severely over-deformed tunnels.  
186 Based on the statistics of accidents that occurred to the Shanghai metro tunnels  
187 (Huang and Zhang, 2016), the unexpected extreme surcharge on ground surface is the  
188 most serious factor among all the environmental disturbances causing large tunnel  
189 deformations. Thus, the surcharge is selected as the external environmental  
190 uncertainty. In the robust rehabilitation design, the surcharge is simulated by applying  
191 pressure to the ground surface above the tunnel within the numerical model. The  
192 whole numerical analysis procedure is as shown in Fig. 4, for simplification purposes,

193 the steps of the initial geostatic stress equilibrium and tunnelling excavation are not  
194 described here, as these have been already finished before this procedure starts. The  
195 numerical analysis includes following three steps: (1) The surcharge  $P_0$  is applied and  
196 the deformation is recorded before the steel plates are added. The horizontal diameter  
197 of the tunnel after this step is denoted as  $D_{h0}$ . The specific value of  $P_0$  is determined  
198 according to the real tunnel conditions. That is to say, the activation trigger of steel  
199 plate and bond spring elements are different from case to case; (2) The steel plate  
200 elements and the bond spring elements between the lining and the steel plates are  
201 activated in this step to simulate the retrofitting of steel plates to deformed segmental  
202 tunnel linings; (3) The surcharge  $P$  is continuously applied in this step. The horizontal  
203 diameter of the tunnel after this step is denoted as  $D_h$ . The change in horizontal  
204 convergence of the tunnel after applying the steel plates is then calculated e.g.,  
205  $\Delta D_{hs} = D_h - D_{h0}$ .

206 Step 4: Based on the proposed numerical model, given the characteristics of the  
207 noise factors and specific values for the design parameters, the mean value and  
208 standard deviation of the reinforced tunnel performance  $\Delta D_{hs}$  need to be evaluated.  
209 Recalling that a smaller variation in performance (i.e. in terms of the standard  
210 deviation) indicates a higher robustness. However, deriving the mean and standard  
211 deviation of the tunnel performance is quite variable, as the performance function for  
212 such a problem is a numerical model without an explicit function. Thus the five-point  
213 point estimate method (5-point-PEM) procedure proposed by [Zhao and Ono \(2000,](#)  
214 [2001\)](#) is adopted here to estimate the mean and standard deviation of  $\Delta D_{hs}$ .

215 Within the proposed 5-point-PEM, the estimating points are obtained in the  
 216 standard normal space. Therefore the random variables ( $x_i$ ) need to be transformed  
 217 into standard normal variables ( $u_i$ ), which can be easily accomplished by the  
 218 *Rosenblatt* transformation (Hohenbichler and Rackwitz, 1981). As for a single  
 219 variable function  $y=y(x)$  the mean and standard deviation of  $y$  can be calculated as  
 220 follows:

$$221 \quad \mu_y = \sum_{j=1}^m P_j y [T^{-1}(u_j)] \quad (1)$$

$$222 \quad \sigma_y = \sqrt{\sum_{j=1}^m P_j (y [T^{-1}(u_j)] - \mu_y)^2} \quad (2)$$

223 Where  $T^{-1}(u_j)$  is the inverse *Rosenblatt* transformation,  $\mu_y$  is the mean value of  $y$ ,  
 224  $\sigma_y$  is the standard deviation of  $y$ . The five estimating points in the standard normal  
 225 space and the corresponding weights are:

$$226 \quad \begin{aligned} u_1 &= 0; P_1 = 8/15 \\ u_2 &= -u_3 = 1.3556262; P_2 = P_3 = 0.2220759 \\ u_4 &= -u_5 = 2.8569700; P_4 = P_5 = 1.12574 \times 10^{-2} \end{aligned} \quad (3)$$

227 For a function of multi variables  $G = G(X)$ , where  $X = x_1, x_2, \dots, x_n$ .

$$228 \quad G_i = G[T^{-1}(U_i)] \quad (4)$$

229 Here  $U_i$  means  $u_i$  is the only random variable with other variables equal to the mean  
 230 values. The mean and standard deviation of  $G$  can be obtained using the following  
 231 equations:

$$232 \quad \mu_G = \sum_{i=1}^n (\mu_i - G_\mu) + G_\mu \quad (5)$$

233 
$$\sigma_G = \sqrt{\sum_{i=1}^n \sigma_i^2} \quad (6)$$

234 Where  $G_\mu$  is the function value when all variables equal to their mean values,  $\mu_i$  and  
 235  $\sigma_i$  are the mean and standard deviation of  $G_i$ , which can be obtained using Eqns. (1)  
 236 and (2). In this study, to evaluate the variation of the reinforced tunnel performance  
 237 caused by multi sources of uncertainties,  $\Delta D_{hs}$  could be represented by  $G$ , and the  
 238 parameter variable vector  $X$  contains the soil Young's modulus ( $E_s$ ) and the ground  
 239 surface surcharge ( $P$ ). The mean and standard deviation of  $\Delta D_{hs}$  can be easily  
 240 calculated by Eqns. (3)-(6). More details of the proposed 5-point-PEM can be found  
 241 in [Zhao and Ono \(2000\)](#).

242 Let  $n$  denote the number of noise factors, therefore  $M=4*n+1$  calculations will  
 243 be required for one set of design parameters using the proposed 5-point-PEM. This  
 244 repetition can be achieved by running the ABAQUS numerical analysis automatically  
 245 in the Matlab environment.

246 Step 5: In this step, the mean value and standard deviations for each of the  $N$   
 247 designs in the design space are obtained by repeating the analysis in Step 4.

248 Step 6: For the purposes of getting the most robust design at low cost, the  
 249 multi-objective optimization algorithm is carried out to yield the Pareto Front in this  
 250 step. Thus there are two objectives in the robust rehabilitation design strategy, one is  
 251 to enhance the robustness of segmental tunnel lining strengthened by steel plates,  
 252 which can be realized by minimizing the standard deviation of  $\Delta D_{hs}$ , and the other one  
 253 is to minimize the rehabilitation cost.

### 254 2.3 Cost evaluation

255 In this study, the total cost of the rehabilitation ( $C$ ) is made up of two main parts,  
256 the cost of the material manufacture ( $C_m$ ) and the cost of the construction and  
257 installation ( $C_c$ ), which are calculated by following equations:

$$258 \quad C = C_m + C_c \quad (7)$$

259 Where  $C_m$  can be further calculated from:

$$260 \quad C_m = p_s \times (2\pi R_i \times w_s \times t_s \times \rho_s) \quad (8)$$

261 Where  $p_s$  is the unit price of the steel;  $R_i$  is the inner radius of segmental tunnel lining;  
262  $w_s$  is the width of the steel plates;  $t_s$  is the thickness of the steel plates;  $\rho_s$  is the density  
263 of the steel. The unit price of the steel and the construction fee for one ring have been  
264 adopted as 30,000 RMB per kilogram and 50,000 RMB respectively, which are based  
265 on prices in Shanghai.

### 266 2.4 Multi-objective optimization

267 In step 6 of the robust design procedure, a multi-objective optimization problem  
268 is established, as shown in Fig. 5. In this case, the constraints contain the lower and  
269 upper bounds of each design parameter. In addition, the safety requirement is also  
270 implemented as a constraint by insuring the safety factors  $f_s$  above a certain level. In  
271 this case, the safety factor  $f_s$  ensuring the safety of the segmental tunnel lining  
272 reinforced by steel plates is calculated deterministically using equation:

$$273 \quad f_s = \frac{\Delta D_{\max}}{\Delta D_{hs,mean}} \quad (8)$$

274 Where  $\Delta D_{hs,mean}$  is the mean value of the change in horizontal convergence calculated

275 with all the noise factors being adopted as their mean values.  $\Delta D_{max}$  denotes the  
276 maximum transverse convergence deformation of tunnel lining strengthened by steel  
277 plates when the bonding failure occurs, i.e. in this case the value is taken as 26mm as  
278 observed in the full-scale test carried out by Zhao et al. (2015). Thus a desired safety  
279 level could be ensured by giving a specific limit to the safety factors ( $f_{sl}$ ).

280 With the confirmed design objectives and constraints, the multi-objective  
281 optimization algorithm was performed to seek the optimal design solutions. In the  
282 general concept of multi-objective optimization, a set of non-dominated solutions, so  
283 called the Pareto Front, is obtained rather than a unique solution optimizing all the  
284 objectives. Within the set on the Pareto Front, none of them is better than any other  
285 with respect to all the objectives, while the designs in this set are superior to all others  
286 in the whole design space. That means, each design in the set on the Pareto Front is  
287 optimal, as no improvement could be accomplished in one objective without  
288 worsening any other objectives (Gong et al., 2014). In this study, the optimal solutions  
289 are obtained by using the Non-dominated Sorting Genetic Algorithm version II  
290 (NSGA- II) (Deb et al., 2002). The Pareto Front obtained from this process provides a  
291 trade-off relationship between the robustness of the reinforced segmental tunnel lining  
292 and the rehabilitation cost. The final design depends on the individual situation, for  
293 example if a desired robustness is required, the most economical design could be  
294 selected from the Pareto Front. Similarly, if the rehabilitation cost needs to be  
295 controlled, the design with the highest robustness level at the given cost limit could be  
296 obtained. Furthermore, if there is no specific requirement about the robustness and

297 financial cost, the concept of a knee point may provide the preferred or suggested  
298 design within the Pareto Front, which will be explicitly illustrated latter.

### 299 **3. Numerical modeling**

300 A rational robust design for rehabilitation by using bonding steel plates to shield  
301 tunnel lining, as introduced previously, requires a well-established numerical model as  
302 a key step in the flowchart. To this end, a two-dimensional finite element model is  
303 proposed in this paper for its merit of considering the uncertain soil behaviour and the  
304 complex interactions between soils and also between lining and steel plates. The  
305 surrounding soil, the tunnel lining, the steel plates and the interactions between each  
306 of those are all properly simulated in this model and verified by full-scale test results  
307 described in the following sections.

#### 308 **3.1 Establishment of model**

309 A typical two-dimensional finite element model is established using the  
310 commercial finite element code ABAQUS as shown in Fig.5. In this model, the tunnel  
311 has an outer diameter  $D_{out}$  of 6.2m. The mesh size of the entire ground model has a  
312 width of 100m and a depth of 50m. The selected mesh width is about 16 times the  
313 outer diameter which avoids the effect from the boundary on the calculations ([Ding et](#)  
314 [al., 2004](#)), and the mesh utilizes 4710 elements. The soil is simulated using a linear  
315 elastic perfectly-plastic model with a Mohr-Coulomb failure criterion. It is noted that  
316 there are a number of soil models that more precisely represent the nonlinear  
317 behaviour of soils. However, it could be always argued that the elastic  
318 perfectly-plastic soil model with a Mohr-Coulomb yield criteria is probably still the



319 most widely used in numerical simulations, in particular when there are uncertain soil  
320 conditions (Mollon et al., 2011; Do et al., 2013). For the Mohr-Coulomb model, the  
321 most critical parameters are soil Young's modulus  $E_s$ , Poisson ratio  $\nu$ , soil friction  
322 angle  $\varphi$  and cohesion  $c$ . The evaluation of these soil parameters is based on the site  
323 investigation report. Table 1 shows the magnitude of these parameters used in this  
324 analysis. The interaction between the tunnel extrados and the surrounding soils is  
325 simulated using the surface-to-surface contact module in ABAQUS.

326 Details of the simulation used for the steel plate strengthened segmental lining is  
327 shown in Fig.7. The lining segments and the steel plates are simulated as different  
328 parts, and assembled together in the calculation, as shown in Fig.7 (a). The behaviour  
329 of the concrete lining and the steel plates are assumed to be linear elastic perfectly  
330 plastic. The properties are given in Table 2. The tunnel segments are modeled using  
331 4-node bilinear elements and the steel plates are modeled using linear planar beam  
332 elements. It should be noted that the width and thickness of the steel plates, being *easy*  
333 *to control* factors in the robust design procedure, could be modified by changing the  
334 cross section geometry as an input for the beam elements.

335 Fig. 7 (b) shows details of the radial joint in the numerical model. A  
336 surface-to-surface contact is assigned to the interface between the segments, with the  
337 coefficient of friction ratio taken as 0.5 (Liu et al., 2014) and the normal behaviour is  
338 a hard contact allowing separation. The tensile and shear characteristics of the joints  
339 are represented by a tangential spring ( $k_{j_\theta}$ ) and a radial spring ( $k_{j_r}$ ). The tangential  
340 spring ( $k_{j_\theta}$ ) is assigned force-deformation relationship as shown in Fig.8 to simulate

341 the nonlinear behaviour of two grade 5.8 straight bolts with diameter of 30mm and  
342 length of 400mm at the longitudinal joint. The stiffness of the radial spring ( $k_{j_r}$ ) is  
343 adopted as  $5 \times 10^8$  N/m (Ding et al., 2004). Hence, the mechanical and deformational  
344 behaviour of the longitudinal joint in the tangential, radial and rotational directions  
345 could be simulated.

346 Zhao (2015) proposed a numerical model based on the beam-spring model to  
347 investigate the nonlinear response of a segmental lining strengthened by epoxy  
348 bonded steel plates. Following their suggestion, the model to simulate the bond  
349 behaviour between steel plates and lining incorporates the spring element with normal  
350 and shear stiffness, as shown in Fig. 7 (c). The springs allow relative displacement  
351 between the connecting nodes in the radial and tangential directions. The shear  
352 stiffness and normal stiffness are taken as 6.5 MPa/mm and 60 MPa/mm, respectively,  
353 according to the research on epoxy bonded interfaces conducted by Adhikary (2002).  
354 Thus the specific stiffness values of the spring elements can be determined according  
355 to the element numbers of the spring elements between tunnel lining and steel plates.  
356 In this study, 360 pairs of spring elements are distributed uniformly between the lining  
357 and steel plates. There are two spring elements in each pair, one in the tangential  
358 direction ( $k_{b_\theta}$ ) and the other in the radial direction ( $k_{b_r}$ ). The stiffness values of the  
359 three kinds of linear spring elements,  $k_{j_r}$ ,  $k_{b_\theta}$  and  $k_{b_r}$  respectively, can be found in  
360 Table 3.

### 361 3.2 Model validation

362 The proposed numerical model with the simplifications of the radial joints and

363 bond behaviour between the lining and steel plates needed be validated either via field  
364 data from real case study or from a controlled load test before it could be incorporated  
365 into the robust design procedure. Due to the limited number of well-documented case  
366 studies, a full-scale test carried out by [Zhao et al. \(2015\)](#) is used in this paper. The test  
367 results in terms of tunnel convergence subjected to specific load levels are extracted  
368 for validation.

369 Since the full-scale load test carried out by [Zhao et al \(2015\)](#) is a purely  
370 structural test, the soil continuum in the numerical model is not included in this  
371 validation. However, the main simplification in the numerical model is the application  
372 of the spring element both for the radial joints and the bonding behaviour between the  
373 lining and steel plates. Hence, numerically modelling the load structural test was  
374 considered sufficient to validate the rationality for the above assumptions.

375 The test was based on a typical Shanghai metro segmental tunnel lining with  
376 15m overburden of soil, the dimension of which was same with that shown in Fig.2.  
377 As shown in Fig. 9, 24 point loads were applied to the external surface of the tunnel  
378 lining, which were divided into three groups with different values, P1 (6 loading  
379 points), P2 (10 loading points), and P3 (8 loading points). The relative displacement  
380 between the top and bottom of the tunnel lining ( $\Delta D_v = D_v - D_v'$ ), i.e. called the vertical  
381 convergence, was adopted herein as the indicator of overall deformational response of  
382 segmental tunnel linings. As illustrated in Fig. 10, there are three steps for the whole  
383 loading process: (1)  $P_2 = P_1 \times 0.65$ ,  $P_3 = 0.5 \times (P_1 + P_2)$ , loaded until P2 equals to the  
384 passive earth pressure 275kN; (2)  $P_2 = 275\text{kN}$ ,  $P_3 = 0.5 \times (P_1 + P_2)$ , loading continued

385 until  $\Delta D_v$  is approximately 120mm, the steel plate beam elements and bond spring  
386 elements are active at this point to simulated the application of the steel plates; (3)  
387  $P_2=275\text{kN}$ ,  $P_3=0.5 \times (P_1+P_2)$ , loading then continued until  $P_1=600\text{kN}$ . In the  
388 numerical simulations, the load steps and the size of the tunnel lining and steel plates  
389 are the same as those used in the test. Further details can be found in [Zhao et al.](#)  
390 [\(2015\)](#).

391 The calculated deformational responses from the numerical model were extracted  
392 and compared to the experimental results. Fig.10 illustrates the vertical convergence  
393 ( $\Delta D_v$ ) against  $P_1$  from both the full-scale test (dotted line) and the numerical analysis  
394 (solid line). The deformation of the segmental lining at two stages, i.e. the initial earth  
395 pressure loading and the loading after the bonding of the steel plates are both captured  
396 by the loading test and numerical analysis. In the first stage, it is observed from the  
397 physical and numerical results that the tunnel deformed nonlinearly with an increase  
398 in the surrounding load. Obviously, this is due to the nonlinearity of the joints springs  
399 and the geometric nonlinearity of the assembled segmental linings. A maximum  
400 difference in  $P_1$  between the full-scale test and the numerical analysis is  
401 approximately 4.8%, which indicates good agreement even for the largest discrepancy.  
402 In the next stage, the deformed segmental linings is reinforced by the steel plates. At  
403 this stage the load  $P_1$  is shared by both the lining and the steel plates together. An  
404 immediately inflection appears right after the reinforcement, as shown in Fig.11,  
405 which proves a significant improvement in the stiffness of the segmental lining due to  
406 steel plate reinforcement. A maximum difference of 2.9% is observed between the two

407 results when P1 reaches 580kN. However, it should be noted that the failure of  
408 segmental lining reinforced by epoxy bonded steel plates cannot be captured by the  
409 proposed numerical model since the bonding springs behave linearly. Although, since  
410 there is a good agreement between the two results, it was proposed the numerical  
411 model could be used for the subsequent deformation analysis of the segmental lining  
412 strengthened by bonded steel plates.

#### 413 **4. Application of robust retrofitting design to a case study**

##### 414 **4.1 Case study information**

415 To illustrate the proposed robust retrofitting design methodology, a repair project  
416 of an operational shield tunnel disrupted by an extreme surcharge on the ground  
417 surface is introduced, and the proposed robust design methodology is applied to the  
418 design for steel plate rehabilitation in this case. As reported by [Huang and Zhang](#)  
419 [\(2016\)](#), and as shown in Fig.12, a large amount of soil was found to be deposited on  
420 the ground surface without permission along the alignment of tunnel of the east  
421 extension line of the Shanghai metro line 2. The tunnel had been driven through layers  
422 consisting typical Shanghai soft clays, i.e. muddy and silty clays. The cross section of  
423 the tunnel is the same as that shown in Fig.1, and the longitudinal joints of the  
424 segmental lining were arranged in straight lines. The cover depth of this tunnel is  
425 15~20m. The deposited soil had a height ranging from 2m to 7m creating a large  
426 surcharge on the ground surface. The segmental tunnel lining underneath this load  
427 area was badly damaged, with a large number of defects, such as lining deformation,  
428 cracks and water leakage being detected and threatening the safety of the metro

429 operation. Details of the geological conditions and the tunnel information can be  
430 found in [Huang et al. \(2017\)](#).

431 As for the emergency response to this accident, a series of rehabilitation methods  
432 were applied in the repair work of the damaged tunnel. The lining segment rings from  
433 No.500 to No.600 were reinforced using epoxy bonded steel plates. The steel plates  
434 had a width of 850mm and thickness of 30mm and were chosen in this case based on  
435 practical experience.

#### 436 **4.2 Parameters**

437 The robust design methodology has been subsequently applied to the design of  
438 the steel plate rehabilitation for the damaged segmental lined tunnel in this case. The  
439 parameters to be used within the numerical model for the proposed design  
440 methodology needed to be determined. The properties of the segmental tunnel lining  
441 are shown in Table 1. The ground was simplified to homogenous and the  
442 geotechnical parameters of the soil were adopted based on the site conditions. As  
443 introduced previously, an elastic perfectly plastic constitutive model with a  
444 Mohr-Coulomb failure criteria were assigned to the ground soil within the proposed  
445 numerical model, with the soil stiffness being indicated by Young's modulus ( $E_s$ )  
446 while the soil strength was given by friction angle ( $\varphi$ ) and cohesion ( $c$ ). Since the  
447 variance in the stiffness parameters was more influential than the strength parameters  
448 to the tunnel lining deformation, which was of more interest for the robustness  
449 analysis, the friction angle ( $\varphi$ ) and cohesion ( $c$ ) were adopted as deterministic values  
450 according to the site investigation given by [Huang et al. \(2017\)](#), while the Young's

451 modulus ( $E_s$ ) was treated as a random variable following lognormal distribution with  
452 a mean of 20MPa and a coefficient of variance ( $COV$ ) of 0.3.

453 The height of the deposited soil within the surcharged area was on average 5m,  
454 and assuming that the unit weight of the deposited soil was  $20\text{kN/m}^3$ , the value of the  
455 surcharge before reinforcement ( $P_0$ ) was taken as 100kPa. In this case, the surcharge  
456 after reinforcement ( $P$ ) was treated as a random variable following a lognormal  
457 distribution with a mean of 50kPa and a  $COV$  of 0.4, although it should be noted that  
458 the characteristic value of  $P$  will be different from case to case and should be  
459 determined according to the design requirements.

460 As introduced previously, the width  $w_s$  and thickness  $t_s$  of the reinforcing steel  
461 plates are design parameters. Considering the manufacturing convenience of steel  
462 plates and engineering experience, the range of  $w_s$  was taken from 700mm to 1200mm  
463 in increments of 50mm and the range of  $t_s$  was taken from 5mm to 30mm in  
464 increments of 2.5mm. As for the cost evaluation of steel plate rehabilitation, the  
465 construction fee of steel plate rehabilitation for one ring  $C_c$  was adopted as 50,000  
466 RMB, and the unit price of the steel  $p_s$  was adopted as 30,000 RMB/t in this case. As  
467 for the safety requirement, the ultimate horizontal convergence of the reinforced  
468 segmental lining was adopted as  $\Delta D_{max}$ , the safety factor ( $f_s$ ) was limited to be higher  
469 than 1.5 to ensure the safety of segmental tunnel linings reinforced with bonded steel  
470 plates in the future.

### 471 **4.3 Parametric analysis**

472 Before conducting the robust design for the rehabilitation of segmental tunnel

473 lining using steel plates, a parametric analysis was conducted to investigate the  
474 influence of the noise factors ( $E_s$  and  $P$ ) and the design parameters ( $w_s$  and  $t_s$ ) on the  
475 design objectives.

476 In order to illustrate the influence of the soil properties and surcharge value on  
477 the segmental tunnel lining performance, the curves of horizontal convergence against  
478 surcharge value of tunnel under different conditions are presented in Fig. 13.  
479 Comparing the curves for the steel plate reinforced segmental tunnel lining and the  
480 one without any treatment, the stiffness is significantly improved due to the  
481 reinforcement. For the curves where the soil Young's modulus was taken as mean  $E_\mu$ ,  
482 the gradient of curve changes from 1.208 to 6.923, which indicates the stiffness of the  
483 reinforced tunnel is 5.7 times higher than that of the tunnel without reinforcement.  
484 Moreover, by comparing the curves for all the soil Young's modulus values, i.e.  
485  $E_{\mu-\sigma}$ ,  $E_\mu$  and  $E_{\mu+\sigma}$ , it is obvious that the variance in this soil property has an impact on  
486 the horizontal convergence. Nevertheless the degree of variation is significantly  
487 reduced due to the steel plates, which means the robustness of the segmental tunnel  
488 lining could be enhanced to a large degree by bonding steel plates to it.

489 For the purposes of showing how the design parameters influence the robustness  
490 and cost of segmental tunnel lining reinforced by steel plates, the relationship between  
491 sizes of steel plates and design cost and robustness are presented in Fig. 14. It is  
492 evident that the standard deviation decreases with increase in the steel plate width ( $w_s$ )  
493 or thickness ( $t_s$ ). In addition, comparing the design with  $w_s=1000\text{mm}$  and  $t_s=20\text{mm}$  in  
494 Fig.14 (a) and the design with  $w_s=800\text{mm}$  and  $t_s=25\text{mm}$  in Fig.14 (b), the calculated



495 costs of the steel plate rehabilitation are both 131,340 RMB, while the standard  
496 deviation (std) of  $\Delta D_{hs}$  are 1.864 and 1.816 respectively. The cost of the two designs  
497 are the same, however the latter one shows a higher level of robustness. This means  
498 that the increase in investment could bring about a higher level of robustness, however,  
499 the robustness may sometimes be different even with for same cost. Therefore, the  
500 optimization shows its importance within the robust design procedure.

#### 501 **4.4 Robust retrofitting design**

502 In this example of the robust retrofitting design procedure, the elastic modulus of  
503 soil ( $E_s$ ) and the surcharge after reinforcement ( $P$ ) are the noise factors, while height  
504 ( $w_s$ ) and thickness ( $t_s$ ) of reinforcing steel plates are the design parameters. From the  
505 parameters introduced previously, the design constraints can be confirmed to include  
506 the lower and upper bound of the design parameters and the safety requirement. One  
507 of the design objectives is to maximize the design robustness by minimizing the  
508 standard deviation of  $\Delta D_{hs}$ , however, the other one is to minimizing the cost of the  
509 steel plate rehabilitation. Thus the process of the robust design for rehabilitation of  
510 segmental tunnel linings using steel plates is carried out as a multi-objective  
511 optimization problem as illustrated in Fig. 15. The Non-dominated Sorting Genetic  
512 Algorithm version II (*NSGA- II*) (Deb et al., 2002) has been employed to obtain the  
513 Pareto Front for the established multi-objective model.

514 As shown in Fig. 16, the Pareto Front obtained using NSGA- II is marked as  
515 hollow circles within the two-dimensional coordinates, where two objectives, the  
516 standard deviation of  $\Delta D_{hs}$  and cost, are in x and y axes respectively. Within the

517 obtained Pareto Front, it is obvious that the robustness tends to increase as the total  
518 cost increases, which means that increasing the investment can significantly improve  
519 the design robustness. Between all these designs on the Pareto Front, none of them is  
520 better than any other in all the objectives, which offers a trade-off relationship  
521 between to objectives of robustness and cost. It should be noted that, all the designs  
522 on the Pareto Front satisfy the safety requirement.

523 The obtained designs in the existing Pareto Front are such that a choice of the  
524 most optimal single design is not straightforward. Thus engineers need make decision  
525 with the help of the trade-off relationship between design robustness and cost.  
526 However, the most preferred or recommended design named the ‘knee point’ can be  
527 obtained in such a bi-objective problem by using a multi-criteria decision making  
528 methodology (Kalyanmoy and Shivam, 2011). A knee point is almost the most  
529 preferred design, since a small improvement in any one objective requires an  
530 unfavorably large sacrifice in another. The normal boundary intersection method has  
531 been adopted herein to locate the knee point on the obtained Pareto Front (Das 1999;  
532 Juang et al., 2014). In this method, as shown in Fig. 16, two extreme points  $A$  and  $B$   
533 are obtained to construct the boundary line  $L(A,B)$ . Subsequently, for each design  
534 point on the Pareto Front, the distance from the boundary line  $L(A,B)$  can be  
535 calculated. Thereafter, the design point with the maximum distance from the boundary  
536 line  $L(A,B)$  is defined as the knee point. In this example, the knee point has the  
537 following parameters:  $w_s=750\text{mm}$ ,  $t_s=15\text{mm}$  with a cost of  $9.575\times 10^4$  RMB. Above  
538 this level, a small improvement in robustness may need a large involvement. While

539 below this level, a slight cost decrease will significantly reduce the design robustness.

540 In Fig. 17, design 1 represents the actual design in this case, designs 2 and 3 are  
541 the two design point within the obtained Pareto Front, and design 4 is the design  
542 yielded by using concept of the knee point. A comparison of these four designs is  
543 shown in Table 4. Compared with design 1, the robustness of design 2 is enhanced  
544 with little increase in cost, while design 3 yields almost the same robustness with a  
545 lower cost. Although the robustness of design 4 is lower than that of design 1, the cost  
546 saving is large. Therefore, the significance of the robust retrofitting design proposed  
547 in this paper is that the design can be carried out considering both the highest  
548 robustness and the lowest cost simultaneously.

## 549 **5. Conclusion**

550 This paper has presented a general framework for the robust retrofitting design  
551 methodology of segmental lined tunnel of shield tunnels using steel plates. The goal  
552 of the proposed design methodology is to enhance the robustness of the reinforced  
553 segmental tunnel lining against the design uncertainties with respect to achieving low  
554 cost, which can be accomplished by varying the design parameters to minimize the  
555 variation of the reinforced tunnel performance given some uncertain level in  
556 surrounding environments. Specifically, the bonding of steel plates to the lining is  
557 selected as a typical example of such a kind of rehabilitation design discussed in this  
558 paper. The general framework of the robust design method is initially presented. Then  
559 a two-dimensional finite element model is established to simulate the steel plates  
560 retrofitting for deformed segmental tunnel linings. The interactions between the steel

561 plates and the lining and also between the lining and the ground soil are carefully  
562 modelled and verified by the full-scale load test results. Finally, a detailed design  
563 example is carried out for the applicability of the purposed robust design methodology  
564 for rehabilitation of segmental tunnel linings by using steel plates. The results  
565 presented in this paper demonstrate the significant potential of utilizing the robust  
566 retrofitting design methodology combined with the multi-objective optimization  
567 technique where decisions involve different design options and cost. The following  
568 conclusions can be draw:

569 (1) The proposed numerical model was able to simulate the steel plate reinforcement  
570 procedure and the structural response of segmental tunnel linings. The deformation of  
571 the segmental linings develops nonlinearly with an increase in surcharge loading on  
572 the ground surface. The overall stiffness of the segmental lining can be significantly  
573 improved due to the installation of steel plates. The uncertainties existing in the  
574 surrounding environment, e.g. the soil conditions and the ground surface surcharge,  
575 may cause a variation in the performance of the reinforced segmental tunnel lining.

576 (2) The concept of the robust retrofitting design methodology is introduced in this  
577 article, where in this case the design is considered to be robust if the reinforced tunnel  
578 performance is insensitive to the variation in the noise factors (in this case, the soil  
579 conditions and ground surcharge). The proposed design method is accomplished by  
580 varying the design parameters to minimize the standard deviation of reinforced tunnel  
581 performance and the cost simultaneously using a multi-objective optimization  
582 algorithm.

583 (3) The Pareto Front derived from the multi-objective optimization reveals trade-off  
584 relationships between the design robustness and the rehabilitation cost. Comparing all  
585 the designs within the obtained Pareto Front, none is better than any other in  
586 achieving all the objectives, and the engineer can make decisions with respect to their  
587 own financial restraints or robustness goals. Nevertheless, the most preferred or  
588 recommended design could be pointed out with the concept of the knee point.

589 It should be noted that the robust retrofitting design methodology presented in this  
590 paper is a potentially powerful tool that can be applied not only for tunnel linings, but  
591 also for other underground or above ground structures. However, the details may be  
592 different from case to case. For example, the standard deviation of the tunnel  
593 transverse deformation is adopted to indicate the sensitivity to the noise factors in this  
594 paper, while the appropriate sensitivity index needs to be selected for a different  
595 problem. In addition, in this paper the retrofitting cost is calculated according to the  
596 volume of reinforcing steel plate. However, the evaluation of the retrofitting cost may  
597 be more precisely represented in other situations by considering the influence of, for  
598 example, time. Therefore, further investigation needs to be conducted when adopting  
599 this method for solving other geotechnical or structural problems.

## 600 **Acknowledgements**

601 This study is substantially supported by the Natural Science Foundation Committee  
602 Program (No. 51538009, 51608380), by Shanghai Rising-Star Program  
603 (17QC1400300), by International Research Cooperation Project of Shanghai Science  
604 and Technology Committee (No. 15220721600), by the Shanghai Science and

605 Technology Committee Program (No. 17DZ1204205) and by Peak Discipline  
606 Construction on Civil Engineering of Shanghai Project. Hereby, the authors are  
607 grateful to these programs.

608

609 **Reference:**

- 610 Abaqus. Abaqus User's Manual, Version 6.10. Dassault Systèmes, 2010
- 611 Adhikary, B. B., & Mutsuyoshi, H., 2002. Numerical simulation of steel-plate strengthened  
612 concrete beam by a non-linear finite element method model. *Construction & Building*  
613 *Materials*, 16(5), 291-301.
- 614 Beer, M., & Liebscher, M., 2008. Designing robust structures – a nonlinear simulation based  
615 approach. *Computers & Structures*, 86(10), 1102-1122.
- 616 Chang, C. T., Sun, C. W., Duann, S. W., & Hwang, R. N., 2001. Response of a taipei rapid  
617 transit system (trts) tunnel to adjacent excavation. *Tunnelling & Underground Space*  
618 *Technology*, 16(3), 151-158.
- 619 Chang, C. T., Wang, M. J., Chang, C. T., & Sun, C. W., 2001. Repair of displaced shield  
620 tunnel of the taipei rapid transit system. *Tunnelling & Underground Space Technology*,  
621 16(3), 167-173.
- 622 Das, I., 1999. On characterizing the “knee” of the pareto curve based on normal-boundary  
623 intersection. *Structural Optimization*, 18(2-3), 107-115.
- 624 Deb, K., Pratap, A., Agarwal, S., & Meyarivan, T., 2002. A fast and elitist multiobjective  
625 genetic algorithm: nsga-ii. *IEEE Transactions on Evolutionary Computation*, 6(2),  
626 182-197.
- 627 Ding, W. Q., Yue, Z. Q., Tham, L. G., Zhu, H. H., Lee, C. F., & Hashimoto, T., 2004. Analysis  
628 of shield tunnel. *International Journal for Numerical & Analytical Methods in*  
629 *Geomechanics*, 28(1), 57-91.
- 630 Doltsinis, I., & Zhan, K., 2004. Robust design of structures using optimization methods.  
631 *Computer Methods in Applied Mechanics & Engineering*, 193(23–26), 2221-2237.
- 632 DGJ08-11, 2010. Shanghai foundation design code (DGJ08-11-2010). Shanghai: Shanghai  
633 Construction Committee. (in Chinese).
- 634 Do, N. A., Dias, D., Oreste, P., & Djeran-Maigre, I., 2013. 2D numerical investigation of  
635 segmental tunnel lining behavior. *Tunnelling & Underground Space Technology*, 37(6),  
636 115-127.
- 637 Do, N. A., Dias, D., Oreste, P., & Djeran - Maigre, I. 2015. A new numerical approach to the  
638 hyperstatic reaction method for segmental tunnel linings. *International Journal for*  
639 *Numerical & Analytical Methods in Geomechanics*, 38(15), 1617-1632.
- 640 Gong, W., Wang, L., Juang, C. H., Zhang, J., & Huang, H., 2014. Robust geotechnical design

641 of shield-driven tunnels. *Computers & Geotechnics*, 56(1), 191-201.

642 Gong, W., Huang, H., Juang, C. H., Atamturktur, S., & Brownlow, A., 2014. Improved shield  
643 tunnel design methodology incorporating design robustness. *Canadian Geotechnical*  
644 *Journal*, 52(10), 150226181849001.

645 Hohenbichler, M., and Rackwitz, R., 1981. “Non-normal dependent vectors in structural  
646 safety.” *J. Engrg. Mech., ASCE*, 107(6), 1227–1238.

647 Huang, H. W., & Zhang, D. M., 2016. Resilience analysis of shield tunnel lining under  
648 extreme surcharge: characterization and field application. *Tunnelling & Underground*  
649 *Space Technology*, 51, 301-312.

650 Shao, H., Huang, H. W., Zhang, D. M., & Wang, R. L., 2016. Case study on repair work for  
651 excessively deformed shield tunnel under accidental surface surcharge in soft clay.  
652 *Chinese Journal of Geotechnical Engineering*. (in Chinese)

653 Huang, H.W., Shao, H., Zhang, D., & Wang, F., 2017. Deformational responses of operated  
654 shield tunnel to extreme surcharge: a case study. *Structure & Infrastructure Engineering*,  
655 1-16.

656 Juang, C. H., & Wang, L., 2013. Reliability-based robust geotechnical design of spread  
657 foundations using multi-objective genetic algorithm. *Computers & Geotechnics*, 48(4),  
658 96–106.

659 Juang, C. H., Wang, L., Liu, Z., Ravichandran, N., Huang, H., & Zhang, J., 2013. Robust  
660 geotechnical design of drilled shafts in sand: new design perspective. *Journal of*  
661 *Geotechnical & Geoenvironmental Engineering*, 139(12), 2007-2019.

662 Juang, C. H., Wang, L., Hsieh, H. S., & Atamturktur, S., 2014. Robust geotechnical design of  
663 braced excavations in clays. *Structural Safety*, 49, 37-44.

664 Phoon, K. K., & Kulhawy, F. H., 1999. Characterization of geotechnical variability.  
665 *Foundation Engineering in the Face of Uncertainty@Honoring Fred H. Kulhawy* (Vol.36,  
666 pp.612-624). ASCE.

667 Kiriya, K., Kakizaki, M., Takabayashi, T., Hirose, N., Takeuchi, T., & Hajohta, H., et al.,  
668 2005. Structure and construction examples of tunnel reinforcement method using thin steel  
669 panels. *Nippon Steel Technical Report* (92), 45-50.

670 Kasper, T., & Meschke, G., 2006. A numerical study of the effect of soil and grout material  
671 properties and cover depth in shield tunnelling. *Computers & Geotechnics*, 33(4-5),  
672 234-247.

673 Kwokleung Tsui., 2007. An overview of taguchi method and newly developed statistical  
674 methods for robust design. *Iie Transactions*, 24(5), 44-57.



675 Kalyanmoy Deb, & Shivam Gupta., 2011. Understanding knee points in bicriteria problems  
676 and their implications as preferred solution principles. *Engineering Optimization*, 43(11),  
677 1175-1204.

678 Liu, Z., & Zhang, D., 2014. The mechanism and effects of afpr reinforcement for a shield  
679 tunnel in soft soil. *Modern Tunnelling Technology*, 51(5), 155-160.

680 Liu, C., Zhang, Z., & Regueiro, R. A., 2014. Pile and pile group response to tunnelling using a  
681 large diameter slurry shield – case study in shanghai. *Computers & Geotechnics*, 59(59),  
682 21-43.

683 Mollon, G., Dias, D., Soubra, A. H., & Asce, M. 2011. Probabilistic analysis of pressurized  
684 tunnels against face stability using collocation-based stochastic response surface method.  
685 *Journal of Geotechnical & Geoenvironmental Engineering*, 137(4), 385-397.

686 Ministry of Construction of the People’s Republic of China (MCPRC). Code for design of  
687 strengthening concrete structure (GB50367-2013). China Building Industry Press; 2013 [in  
688 Chinese].

689 Shi, P., & Li, P., 2015. Mechanism of soft ground tunnel defect generation and functional  
690 degradation. *Tunnelling & Underground Space Technology*, 50, 334-344.

691 Taguchi, G., & Wu, Y. I. (1979). Introduction to off-line quality control system. *Journal of*  
692 *Food Protection*, 51(6), 449-451(3).

693 Yuan, Y., Jiang, X., & Liu, X., 2013. Predictive maintenance of shield tunnels. *Tunnelling &*  
694 *Underground Space Technology*, 38(3), 69–86.

695 Ziraba, Y. N., & Baluch, M. H., 1995. Computational model for reinforced concrete beams  
696 strengthened by epoxy bonded steel plates. *Finite Elements in Analysis & Design*, 20(4),  
697 253-271.

698 Zhao, Y. G., & Ono, T., 2000. New point estimates for probability moments. *Journal of*  
699 *Engineering Mechanics*, 126(4), 433-436.

700 Zhao, Y. G., & Ono, T., 2001. Moment methods for structural reliability. *Structural Safety*,  
701 23(1), 47-75.

702 Zhang, D. M., Zou, W. B., & Yan, J. Y., 2014. Effective control of large transverse  
703 deformation of shield tunnels using grouting in soft deposits. *Chinese Journal of*  
704 *Geotechnical Engineering*, 36(12), 2203-2212.

705 Zhang, D.M, Phoon, K. K., Hu, Q.F., & Huang, H.W., 2017. Nonlinear subgrade reaction  
706 solution for circular tunnel lining design. *Canadian Geotechnical Journal*. DOI:  
707 <https://doi.org/10.1139/cgj-2017-0006> (online).

708 Zhao, H., Liu, X., Bao, Y., Yuan, Y., & Bai, Y., 2015. Simplified nonlinear simulation of

709 shield tunnel lining reinforced by epoxy bonded steel plates. *Tunnelling & Underground*  
710 *Space Technology*, 51, 362-371.  
711

712

713

## Table and Figure Captions

714 **Tables:**

715 Table 1 Properties of soil

716 Table 2 Parameters for the segmental tunnel concrete lining and steel plates

717 Table 3 The stiffness values of the spring elements simulating the segmental joints

718 and epoxy bonding behaviour

719 Table 4 Comparison between the actual design and the optimal designs derived by the

720 robust retrofitting design methodology

721 **Figures:**

722 Figure 1 Photograph of a steel plates reinforced segmental tunnel lining

723 Figure 2 Diagram of showing an example of segmental tunnel linings reinforced by

724 steel plates

725 Figure 3 Flowchart for developing a robust retrofitting design

726 Figure 4 Numerical analysis procedure

727 Figure 5 Multi-objective optimization formulation for robust retrofitting design

728 Figure 6 Finite element mesh for the ground

729 Figure 7 Finite element model for steel plates reinforced segmental linings, (a) the 2D

730 model for the full reinforced tunnel lining, (b) the radial lining joint, (c) modelling the

731 bond between the steel plates and the lining segment

732 Figure 8 Force-deformation relationship assigned to tangential spring in the segment

733 joint

734 Figure 9 Schematic of the applied loading

735 Figure 10 The loading process for P1, P2 and P3

736 Figure 11 Comparison between the full-scale test results and the numerical analysis

737 results

738 Figure 12 Location of the surcharge area

739 Figure 13 Curves showing the horizontal convergence ( $\Delta D_h$ ) against surcharge value

740 Figure 14 Influence of steel plate size on cost and robustness, (a) influence of steel

741 plate width ( $w_s$ ), (b) influence of steel plate thickness ( $t_s$ )

742 Figure 15 Formulation of the robust design for the rehabilitation of segmental tunnel

743 linings using steel plates

744 Figure 16 Pareto front obtained using NSGA-II

745 Figure 17 Comparison between the actual design and the optimal designs on the

746 Pareto Front

747

748

749

Table 1 Properties of soil (Huang et al., 2017)

<b>Parameters</b>	<b>Symbol</b>	<b>Unit</b>	<b>Value (or mean value)</b>	<b>COV</b>	<b>Distribution</b>
Poisson's ratio	$\nu$	-	0.167	-	-
Unit weight	$\gamma$	kN/m <sup>3</sup>	18	-	-
Cohesion	$c$	kPa	15	-	-
Friction angle	$\varphi$	°	15	-	-
Young's modulus	$E_s$	MPa	20	0.3	Lognormal

750

751

752

Table 2 Parameters for the segmental tunnel concrete lining and steel plates

	Young's modulus /MPa	Poisson's ratio	Yielding stress /MPa
C55 concrete	35.5	0.167	25.3
steel plates	$2 \times 10^5$	0.2	215

753

754

755 Table 3 The stiffness values of the spring elements simulating the segmental joints

756 and epoxy bonding behaviour

Position	Direction	Symbol	stiffness (N/m)
segmental joints	radial	$k_{j,r}$	$5 \times 10^8$
epoxy bonding	tangential	$k_{b,\theta}$	$3.74 \times 10^8$
	radial	$k_{b,r}$	$3.45 \times 10^9$

757

758

759

760 Table 4 Comparison between the actual design and the optimal designs derived by the

761 robust retrofitting design methodology

<b>Design Point</b>	<b><math>w_s</math> /mm</b>	<b><math>t_s</math> /mm</b>	<b>std of <math>\Delta D_{hs}</math> /mm</b>	<b>Cost / <math>\times 10^4</math></b>
1	850	30	1.800	15.571
2	950	27.5	1.624	15.625
3	750	27.5	1.767	13.388
4	700	17.5	2.324	9.982

762



763



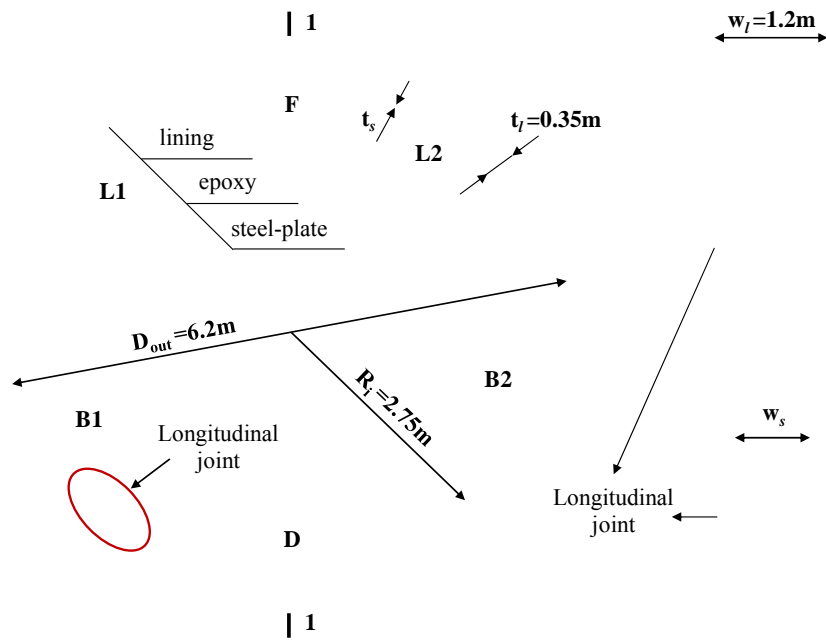
764

765

Figure 1 Photograph of a steel plate reinforced segmental tunnel lining

766

767



768

769 Figure 2 Diagram of showing an example of segmental tunnel linings reinforced by

770

steel plates

771

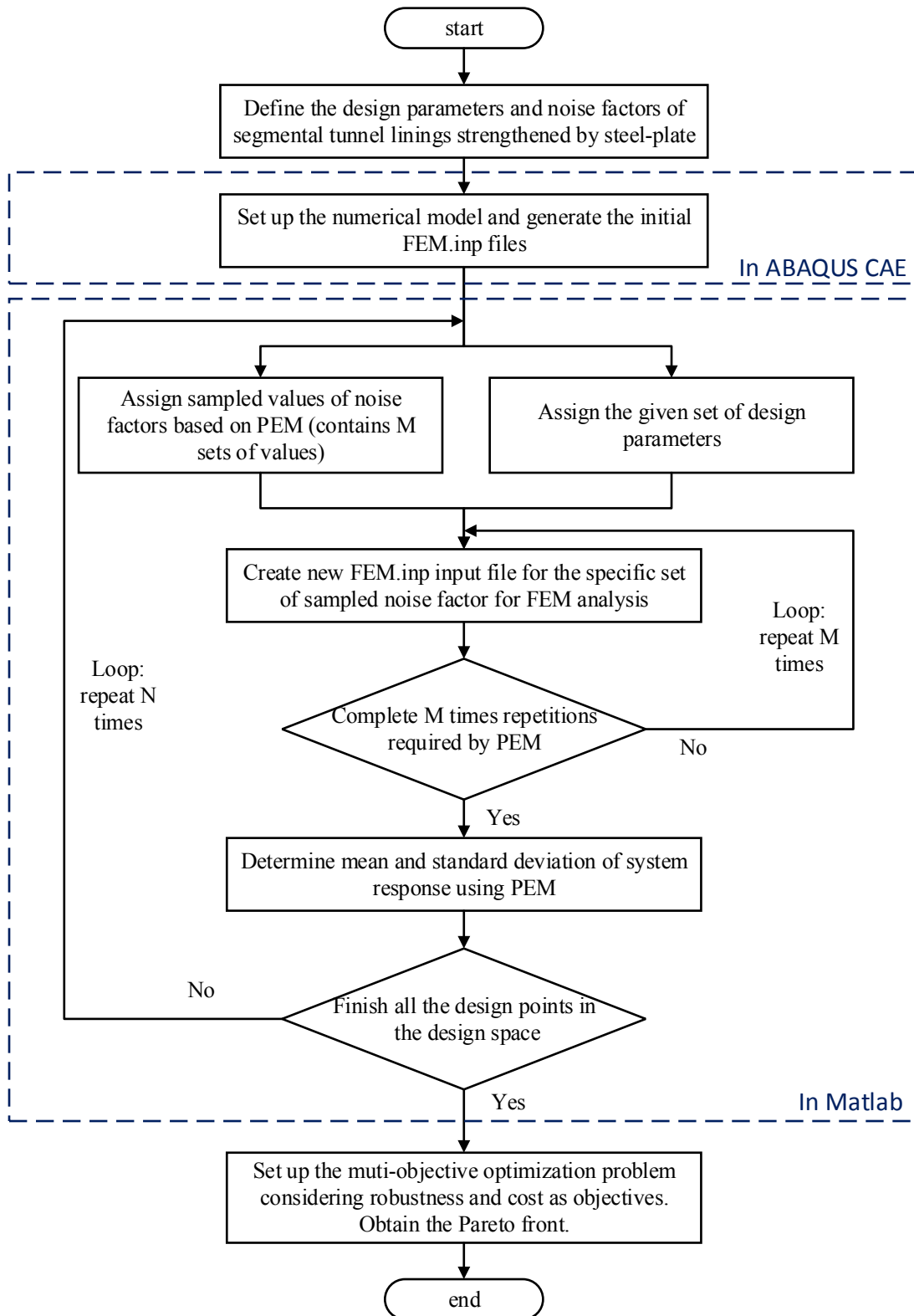
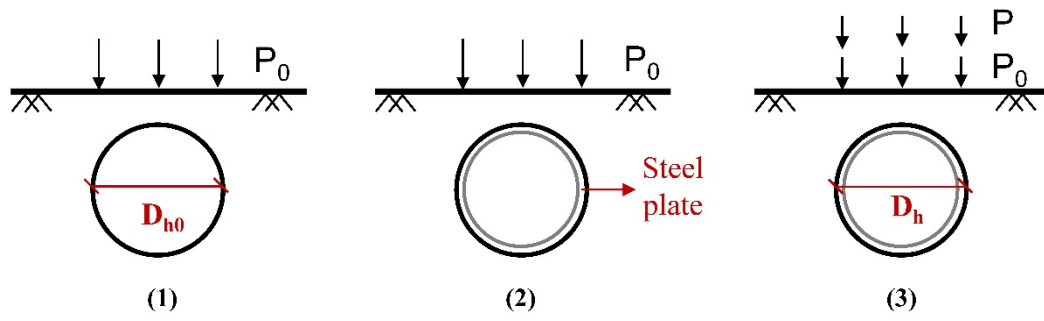


Figure 3 Flowchart for developing a robust retrofitting design

776



777

778

Figure 4 Numerical analysis procedure

779

780

**Find value of design parameters:**  
 $w_s$  (width of reinforcing steel plate)  
 $t_s$  (thickness of reinforcing steel plate)

**Subjected to constraints:**  
 $w_{sl} \leq w_s \leq w_{su}$   
 $t_{sl} \leq t_s \leq t_{su}$   
 $f_s > f_{sl}$

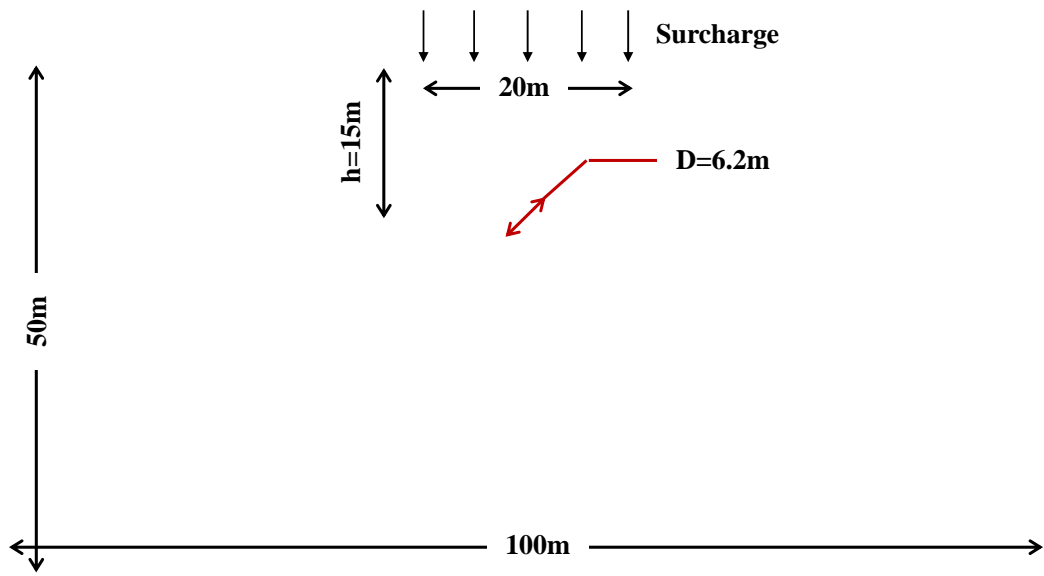
**Objectives:**  
Maximizing the robustness index,  $R_s$   
Minimizing the cost,  $C$

781

782 Figure 5 Multi-objective optimization formulation for robust retrofitting design

783

784



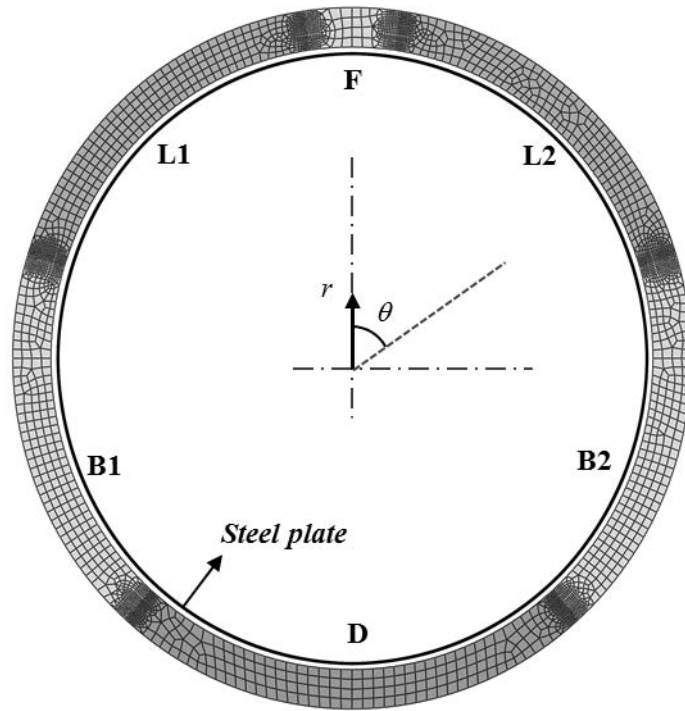
785

786

Figure 6 Finite element mesh for the ground

787

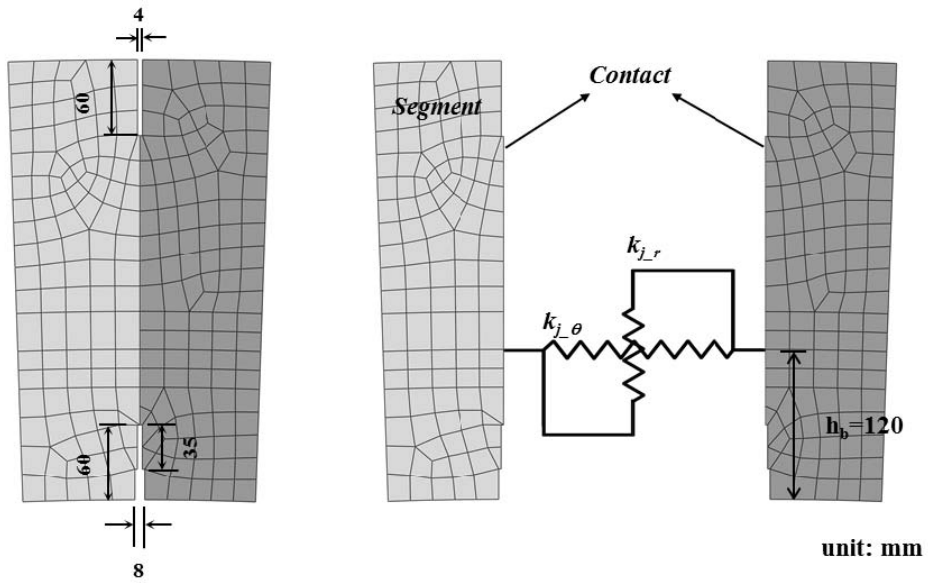
788



789

790

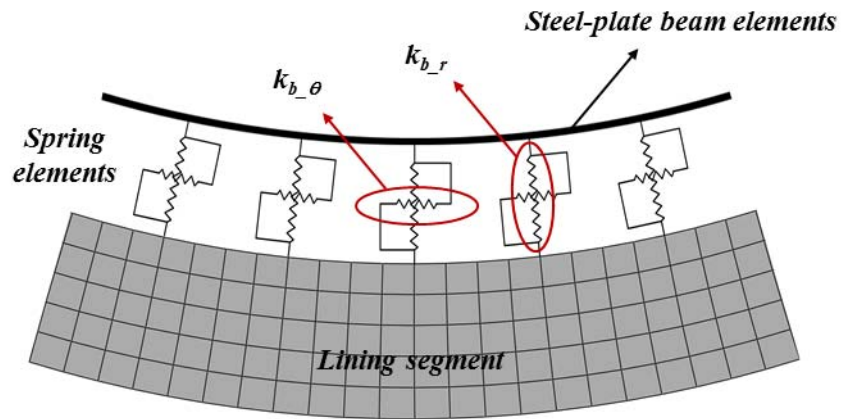
(a)



791

792

(b)



793

794

(c)

795 Figure 7 Finite element model for steel plates reinforced segmental linings, (a) the 2D

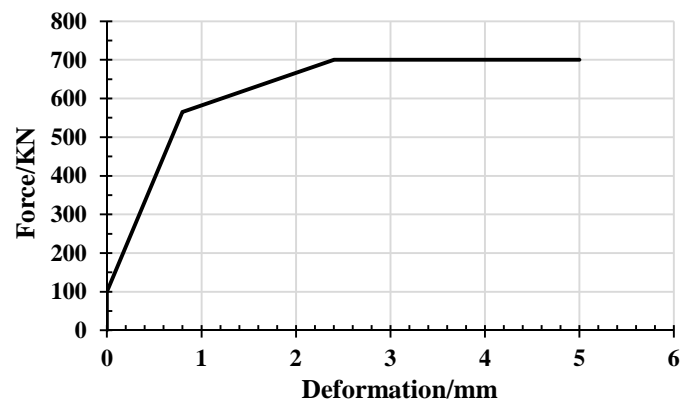
796 model for the full reinforced tunnel lining, (b) the radial lining joint, (c) modelling the

797 bond between the steel plates and the lining segment

798



799



800

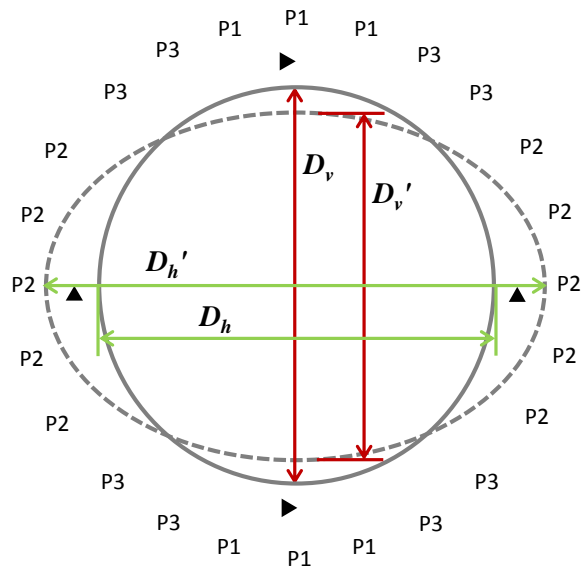
801 Figure 8 Force-deformation relationship assigned to tangential spring in the segment

802

joint

803

804



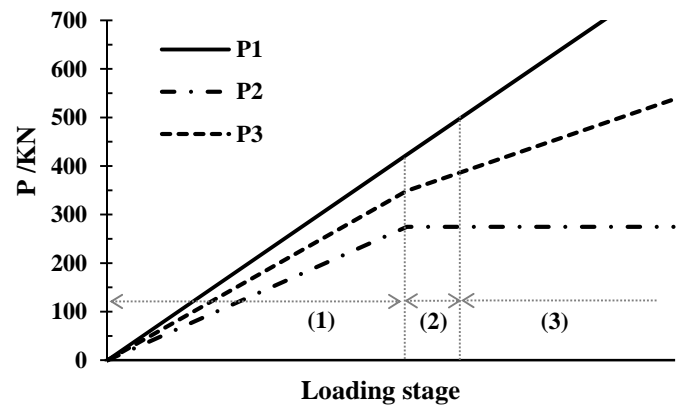
805

806

Figure 9 Schematic of the applied loading

807

808



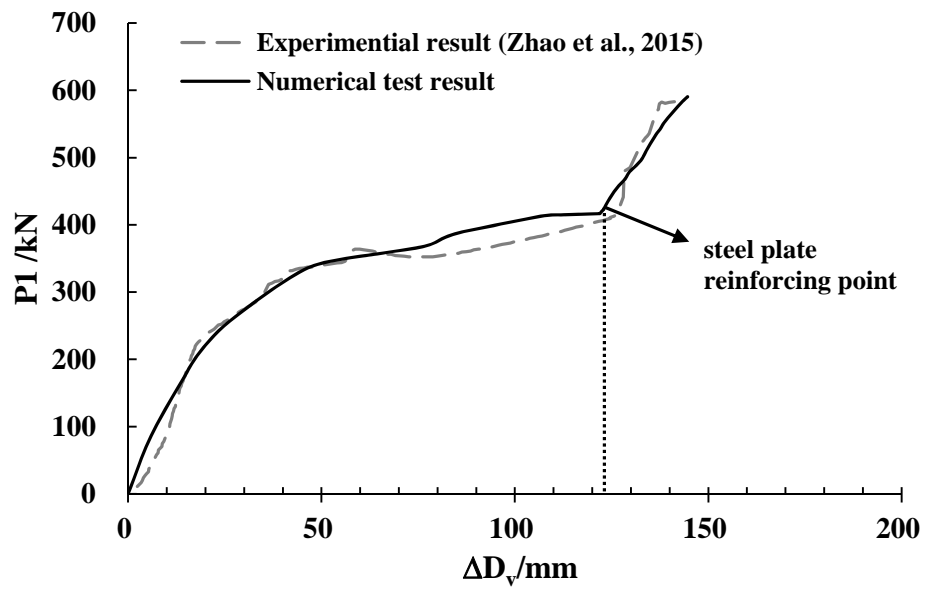
809

810

Figure 10 The loading process for P1, P2 and P3

811

812



813

814 Figure 11 Comparison between the full-scale test results and the numerical analysis

815

results

816

817



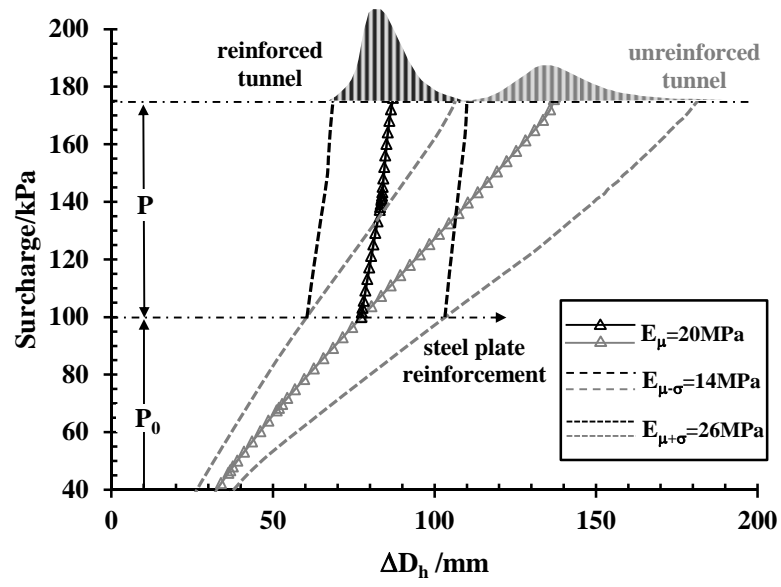
818

819

Figure 12 Location of the surcharge area (Huang et al., 2017)

820

821

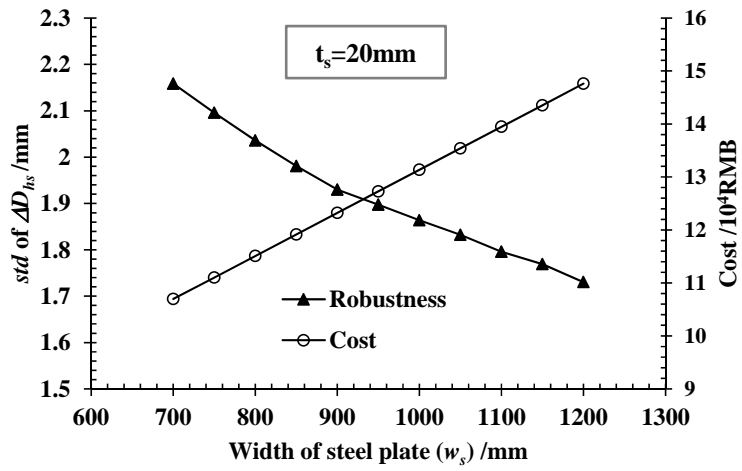


822

823 Figure 13 Curves showing the horizontal convergence ( $\Delta D_h$ ) against surcharge value

824

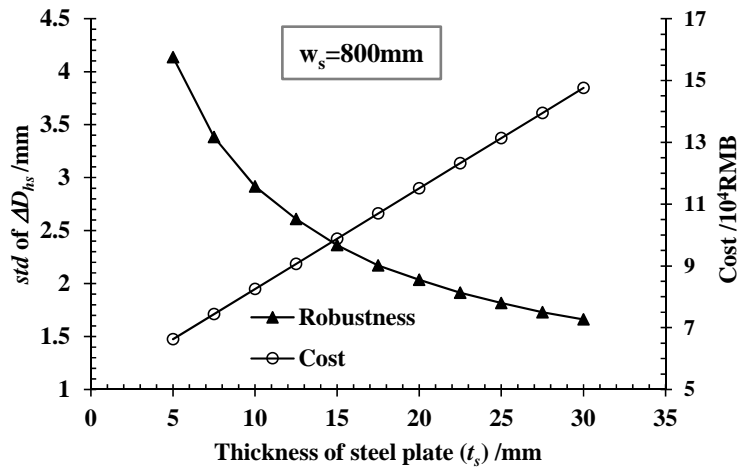
825



826

827

(a)



828

829

(b)

830 Figure 14 Influence of steel plate size on cost and robustness, (a) influence of steel

831 plate width ( $w_s$ ), (b) influence of steel plate thickness ( $t_s$ )

832

833

**Find value of design parameters:**

$w_s$  (width of reinforcing steel plate)

$t_s$  (thickness of reinforcing steel plate)

*unit: mm*

**Subjected to constraints:**

$700 \leq w_s \leq 1200$  (with interval of 50)

$5 \leq t_s \leq 30$  (with interval of 2.5)

Safety factor  $f_s > 1.5$

**Objectives:**

Minimizing the standard deviation of  $\Delta D_{hs}$  (mm)

Minimizing the cost of steel plate reinforcement (RMB)

834

835 Figure 15 Formulation of the robust design for the rehabilitation of segmental tunnel

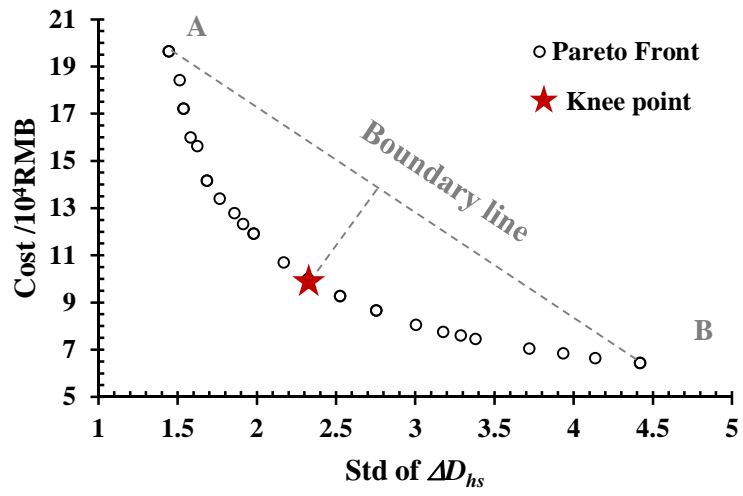
836

linings using steel plates

837



838



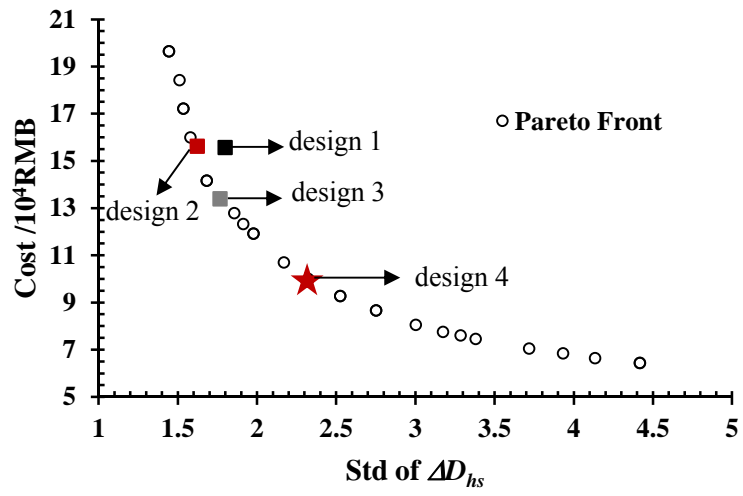
839

840

Figure 16 The Pareto Front obtained using NSGA-II

841

842



843

844 Figure 17 Comparison between the actual design and the optimal designs on the

845

Pareto Front

846